RESEARCH ARTICLE

Development of Piston Materials from Discarded Aluminum Piston Alloyed with Zirconium Diboride and Snailshells

E.O. Olawuni*, M. O. Drowoju, T. B. Asafa, L. O. Mudashiru

Department of Mechanical Engineering, Ladoke Akintola University of Technology, P.M.B. 4000, Ogbomoso, Nigeria.

ABSTRACT: Piston is the major part of an automotive engine. It is commonly produced from aluminum reinforced with expensive particles like graphite, B_4C, TiC and SiC. In most developing nations, used pistons are indiscriminately discarded thereby constituting environmental hazard. To reduce cost of reinforcement and minimize waste disposal challenges, piston materials can be developed from local sources. In this paper, we report the development of piston materials by reinforcing discarded aluminum pistons with zirconium diboride and snailshells. Discarded motorcycle pistons were collected from Ogbomoso Nigeria, melted and then reinforced with zirconium diboride and snailshells at varying proportions based on D-Optimal approach of Design of Experiment. The ingots were then re-cast, machined to standard shapes and characterized for hardness, tensile strength, wear, composition, corrosion rate, fatigue, impact strength among others. These properties were optimized, and the corresponding ingot was further characterized. 75 wt. % aluminum alloy, 15 wt. % zirconium diboride and 10 wt. % snailshells gave the optimal properties with tensile strength, hardness and Young modulus of 148.08 MPa, 99.29 MPa and 18.54 GPa, respectively compared to 47.48 MPa, 78.41 MPa and 9.80 GPa obtained for new aluminum pistons. The wear rate of aluminum alloy reinforced with zirconium diboride and snailshells was 0.021 mm^3/Nm compared to 0.57 mm^3/Nm for new piston. This study has shown that addition of zirconium and snailshells can significantly improve mechanical properties of aluminum.

KEYWORDS: Mechanical Properties, Casting, Aluminum composite, Snailshells, Zirconium diboride.

https://doi.org/10.29294/IJASE.5.1.2018.818-828

1. INTRODUCTION

Aluminum is one of the most versatile of the common light metals. While pure aluminum lacks strength and hardness, it is often alloyed with other elements to increase its strength, conductivity and optical properties for various technological applications [1-2]. Aluminum is a major component of piston, the heart of an engine, and must be light enough to keep inertial loads on moving components to a minimum. Piston is also subjected to cyclic thermal loading and stresses during operation [3]. Pistons technologies continue evolving towards stronger, lighter, thinner and more durable product. Consequently, the mechanical efficiency of engine is expected to rise [3]. Wear and fatigue are the major cause of pistons' damages [4-8]. While wear cannot be eliminated, it can be reduced by selecting appropriate material. Several works have been done on wear behaviours such as the minimization of wear via Taguchi Method [9-10].

Disposal and management of scraps, junk automobile components (like aluminum pistons among others) and snailshells continue to be of critical concern. These wastes are indiscriminately dumped cumulating into landmarks in several major cities in Nigeria. Discarded pistons are considered to be of low economic value, hence they are found in automobile repair shops, dumping sites among others. Studies have shown that snailshells can be used as a low-cost reinforcement for the production of aluminum metal matrix composites for several engineering applications [11-12]. The chemical compositions of snailshells are 97.5wt. % calcium carbonate ($CaCO_3$), calcium phosphate and calcium silicate make the material attractive for reinforcement.

Literature has reported different publications that addressed the problems of piston in terms of fatigue, thermal or mechanical behaviour, wear and mechanical properties [3-10]. Some of the publications were on improving the mechanical properties and comparing the reinforced and unreinforced alloy. Improving mechanical properties of alloy to suit different application constitute a major concern during engineering design. Therefore, this paper will focus on a significant way of improving mechanical properties of a piston at room and high temperature, in order to enhance the thermo-mechanical properties with resistance to shock. It is also paramount to note that high level of discarded motorcycle piston and snailshell dump can be managed and converted to wealth through recycling. The manufacturing technique that will be used is stir cast method because it is simple and cost effective.

To further enhance the mechanical properties of the alloy, zirconium diboride can be added. Zirconium diboride which is known to possess high thermal stability/melting point (used in high temperature applications) retains mechanical strength at high temperature, and will be used as reinforcing materials to overcome the temperature problem which pistons are subjected to during operation. So in addition to waste management and recycling, this study will go a long way to reduce cost of production of piston material. This paper, therefore, reports our experimental results based on reinforcement of discarded aluminum pistons with zirconium diboride and snailshells.

**Corresponding Author: imoleolawuni@gmail.com*

Received: 25.06.2018 **Accepted:** 28.07.2018 **Published on**: 24.08.2018

2. MATERIALS AND METHODS

2.1 Material preparation

Discarded aluminum pistons were collected from auto-mechanic workshops in Ogbomoso, South-West Nigeria. The pistons were cleaned of oil by means of organic solvent and liquid detergent. All the piston scraps were melted in an electric furnace and the molten alloy was obtained as ingot. The compositions of the as-cast samples were analyzed using Energy Dispersive X-ray flourescence Spectrometry (Jiangsu Skyray, EDX 3600B). Several giant African snailshells (*Achatina achatina*) were collected from different locations in Ogbomoso.

Following the work of Jato et al. [11] the snailshells were washed, dried, crushed and grounded. Snailshells obtained were first pulverized into small chips of different geometries and sizes. About 7.6 kg of the pulverized snailshells was ball-milled into 150 μm particles. The ball miller has a capacity of 50 kg, and runs at 50 rpm with power output of 1250 W. Zirconium diboride particles were purchased from local markets, and was used as reinforcing materials to reduce high temperature fatigue because of its ability to retain mechanical strength at high temperature. The melting process was carried out in an oil fired furnace. All the discarded aluminium pistons collected were melted inside a crucible pot in the furnace, hence; the mould was pre-heated and then set to a temperature of 660°C to avoid sudden solidification of the cast samples.

Then 10 wt. % snailshell particles were added to10 wt. % zirconium diboride and later poured into 80 wt. % of piston at melting temperature of 700 ± 5°C and stirred continuously for 5 min. Meanwhile, the temperature of all the mixture was raised to 1300 °C for homogeneity and dross was removed prior to pouring. The procedure was also used for all the samples with varying wt. % and melting was done in an oil-fired furnace.

2.2 Sample preparation

The patterns of the cast rods were made from wood. Each of the rods was sand-cast. Then molten metal collected in form of ingot was poured into the sand mould, left to solidify and removed as cast sample. The sample was then cleaned and inspected for feasible defects. Samples in form of rod of 12 mm diameter and 250 mm length were produced as cast sample. It can then be machined into different specification as required by each test.

2.3 Experimental Design and Optimization

The influences of alloying element on piston performance were studied using D-optimal technique (DOT), which is a component of mixture design of experiment (particle reinforcement aluminum matrix composite). The modified samples involved combinations of aluminum piston, zirconium diboride and snailshells (9 experimental runs) and new piston as control (Table 1). Based on the experimental setup, snaillshells compositions were varied between 0 – 20 wt. % while zirconium compositions were in the range 0 – 30 wt. %. The reinforcements were added to molten aluminum, stirred rigorously to ensure uniformity, and then poured into a mould while unmodified samples which served as control were only re-cast. For each sample, tensile strength (TS) was maximized and wear resistance (WR) was minimized. The samples with the best combination of TS and WR were characterized further.

2.4 Characterization

The microstructure and elemental composition of the samples were obtained using Phenom ProX Scanning Electron Microscope (SEM) equipped with EDX. Tensile and hardness tests were conducted on tensometer (M500-10080 of 100 kW) equipped with compression test accessories of Brinell hardness 500 kef. Moreso, the measurement for Brinell hardness test was repeated thrice and the average values were taken as the result. For the tensile test, the strain rate was 10 mm/min. Prior to test, samples were machined following the ASTM standard for tensile test sample to a required dimension of 10 mm diameter and length 40.00 mm (Figure 1) of testometer testing machine (M500-10080 of 100 KW) equipped with a data acquisition system.

Table 1. Experimental runs obtained from D-optimal technique and control sample

Experimental Run	Al-piston wt. %	Zirconium wt. %	Snailshells wt. %
1	80.00	10.00	10.00
2	80.00	20.00	0.00
3	72.50	22.50	5.00
4	70.00	10.00	20.00
5	75.00	15.00	10.00
6	80.00	0.00	20.00
7	75.00	5.00	20.00
8	70.00	30.00	0.00
9	70.00	20.00	10.00
10	100	New piston	

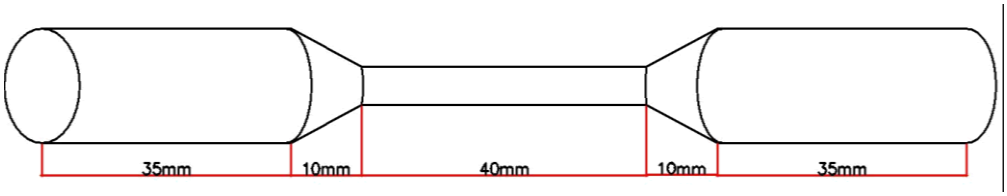

Figure 1: Dimension of the Sample for Tensile Strength Test

The impact strengths of the samples (dimensions of 55 x 10 x 10 mm^3) were obtained using Charpy impact tester with standard V-notch. The impact tests were repeated twice and the average value was taken as the result. The fatigue strengths of the samples were measured using Avery Denison Fatigue testing machine, low fatigue type (Model 7305). The samples were prepared to conform with ASTM standard E 466.

The dry sliding wear behavior of the samples was investigated with a pin-on-disc apparatus. The samples were mounted in the apparatus, and 5 N load was applied so that the stylus pin made a firm contact with the sample. The experiment was carried out with constant load and varying sliding distance. The samples were left to wear for 35 min, after which the sliding distance and the weight loss were measured. The volume loss ΔV was calculated as Equation (1). The wear coefficient which is a measure of wear severity was obtained from Eq. (2),

$$\Delta V = \left(\frac{W_1 - W_2}{\rho} \right) 100\% \qquad \text{Eq. (1)}$$

$$S_r = \frac{\bar{W}}{D_s A_l} \qquad \text{Eq. (2)}$$

where, W_1 and W_2 are weights of the samples before and after wear test, and ρ is the density of the samples, respectively and S_r $\bar{W}$ D_s and A_l denotes specific wear rate, wear volume loss, sliding distance and applied load, respectively.

2.5 Corrosion test

Corrosion test was conducted by potentiodynamic polarization measurements using Tafel method [13]. Prior to each test, samples were grounded and polished using diamond grinders and water based diamond and colloidal silica suspensions of size 0.04 µm. 0.05M NaCl (Panreac), Silver/ Silver chloride (Ag/AgCl), Platinium and samples were used as electrolyte, reference electrode, counter electrode and working electrode, respectively. Then the open circuit potential (OCP) measurements (Tafel polarization) were performed by using a Voltalab PGZ 100 potentiostat. The measurement was carried out between cathodic potential of 0.8 V and anodic domain (OVvs.SCE) with a scan rate of 0.5 mV/s.

3. RESULT AND DISCUSSION

3.1 Tensile strength and Brinell hardness values

Table 2 shows the mechanical properties of the samples as influenced by zirconium diboride and snailshells. Sample 5 (composition: 75 wt. % Al alloy, 15 wt. % ZrB_2, 10 wt. % snailshells) has the highest ultimate tensile strength (148 MPa), Young modulus (18.5 GPa), and modulus of resilience (591 MPa). These values are respectively 212%, 89%, 209% and 414% higher than those obtained from the new piston (control). However, while sample 5 does not have the highest Brinell hardness value, it is 26% higher than the control and Brinell hardness results were obtained in form of average with a standard deviation of 14.28. The yield strengths obtained were 139 MPa for sample 5 and 45 MPa for new piston. Therefore sample 5 was selected as the optimum composition. These results imply that addition of zirconium diboride and snailshells significantly increased the mechanical properties of discarded aluminum piston far beyond those of new piston.

In a similar study conducted by Durowoju and Babatunde [14] in 2014 maximum tensile strength of 82.59 MPa was obtained when recycled Aluminum piston was alloyed with Antimony. Furthermore, maximum hardness and tensile values of 50.8 MPa and 65.01 MPa, were obtained respectively from Manganese dioxide modified recycled Al-332 alloy [15]. Also, Asafa et al. [12] modified discarded motorcycle piston with 16-48 wt. % snailshells particles of size 200-600 µm. It was reported that 48 wt. % snailshells and 600 µm particle size had the optimum hardness and tensile strength of 48.3 MPa and 236.0 MPa, respectively. Meanwhile this study was carried out with a constant particle size of 150 µm and varied wt. % of zirconium diboride and snailshells.

3.2 Wear Test Result

Table 3 shows the various parameters obtained from the wear experiments. It was observed that the weight losses of all the samples are similar with slight differences in their wear rates except for the control sample which has high wear rates. This indicates that the added filler materials reduced the wear rate. The decrease in the wear rate may be attributed to the fact that the filler materials are harder than the base material. As indicated in Table 3, the higher the volume fraction of the filler materials, the lower the specific wear rate which is similar to the results obtained by Saka, et al. [16]. The wear resistance decreased with increased in zirconium diboride. The effect of zirconium diboride was clearly observed compared to the control sample which was not reinforced. Suresha et al. [17] reported that the presence of hard filler materials in polymer materials increase the dry sliding wear resistance

and the decrease in wear rate may be as a result of higher load bearing capacity of hard composite material and a better interfacial bonding between the particle size which lowers particle pull out that leads to higher wear. It is clearly observed in Table 3 that increase in snailshell also reduces the wear rate compared to the control sample which indicates that snailshells is good as a natural filler to reduce wear rate. These results is in complete agreement with those reported by Agunsoye et al. [18] on the effect of silica ceramic particle sizes on the properties of recycled polyethylene composites.

3.3 Further Characterization of the sample with optimal Mechanical Properties

The best sample (sample 5: composition - Aluminum alloy + 15% ZrB_2 + 10% Snail shell) and sample 8 (Aluminum alloy + 30% ZrB_2 + 0% Snail shell), as shown in Table 2, were selected for further characterization using the main criterion for selection of piston material which is high tensile strength because of high compression ratio [3]. Moreso, other mechanical properties are high modulus of elasticity, hardness strength and abrasion resistance.

3.4 Chemical Composition of As-cast and Reinforced Aluminum Alloy

Table 4 shows the material compositions for reinforced and as-cast aluminum samples. The composition of silicon in all the tested samples corroborated the results that conventional piston contains about 25% silicon. Figure 2 shows the EDS of Aluminum alloy reinforced with zirconium diboride and snailshells and as-received control sample.

Table 2. Mechanical Properties of Alloys of used pistons, Zirconium Diboride and Snailshells

No of runs	Specimen	Wt. % AL/ZrB/SS	Ultimate Strength (MPa)	Yield Strength (MPa)	Young Modulus (GPa)	Modulus of Resilience (MPa)	Average Brinell Hardness (MPa)
1	ALZrB_2SS1	80/10/10	69.392	66.200	14.167	169.941	161.135
2	ALZrB_2SS2	80/20/0	79.005	73.800	9.259	337.075	128.220
3	ALZrB_2SS3	72.5/22.5/5	90.438	87.300	10.279	397.837	75.773
4	ALZrB_2SS4	70/10/20	67.660	65.700	16.442	139.210	63.950
5	ALZrB_2SS5	75/15/10	148.078	139.000	18.537	591.423	99.288
6	ALZrB_2SS6	80/0/20	66.871	63.800	12.071	185.233	83.749
7	ALZrB_2SS7	75/5/20	68.717	65.000	16.842	140.183	77.417
8	ALZrB_2SS8	70/30/0	91.228	87.000	17.687	235.277	101.879
9	ALZrB_2SS9	70/20/10	55.131	54.200	17.364	87.520	159.710
10	New Piston	100/0/0	47.479	45.000	9.804	114.970	78.406

Table 3. Wear Resistance Test for Aluminum Alloy, Zirconium diboride and Snailshell with Control sample

S/N	Sample	Wt.% AL/ ZrB/SS	A Initial weight (g)	B Final weight (g)	Ss Sliding Distance (mm)	C = (A-B) Weight loss (g)	$Ws = \frac{\Delta V}{Fn \times Ss}$ Specific wear rate (mm^3/Nm)
1	ALZBSS1	80/10/10	10.352	10.348	8.52	0.004	0.036
2	ALZBSS2	80/20/0	9.925	9.920	8.80	0.005	0.046
3	ALZBSS3	72.5/22.5/5	8.846	8.842	7.63	0.004	0.036
4	ALZBSS4	70/10/20	7.373	7.377	8.27	0.006	0.073
5	ALZBSS5	75/15/10	8.723	8.713	8.73	0.009	0.096
6	ALZBSS6	80/0/20	8.329	8.326	8.58	0.003	0.022
7	ALZBSS7	75/5/20	8.599	8.596	8.75	0.003	0.032
8	ALZBSS8	70/30/0	8.650	8.648	8.70	0.002	0.021
9	ALZBSS9	70/20/10	8.205	8.202	7.83	0.003	0.019
10	CONTROL 1	100/0/0	7.489	7.450	7.39	0.039	0.57

Table 4: Actual composition of the As-cast and reinforced aluminum alloys (wt. %)

Elements	Sample 5	Sample 8	Control 1
Mg	3.7265	0.5366	0.7025
Al	59.6968	68.5185	65.9680
Si	20.2000	19.1643	28.4806
Ti	0.0031	0.1489	0.0128
Cr	0.0595	0.1237	0.0393
Mn	0.3833	0.4985	0.4902
Fe	1.5450	5.4423	1.1483
Ni	0.2197	0.1646	0.0915
Cu	6.6410	2.1569	1.9054
Zn	1.0106	2.8916	0.4002
Sr	0.0241	0.0110	0.0262
Pb	6.2561	0.1525	0.1317
Sn	0.0737	0.1033	0.3615
Sb	0.1505	0.0774	0.2319

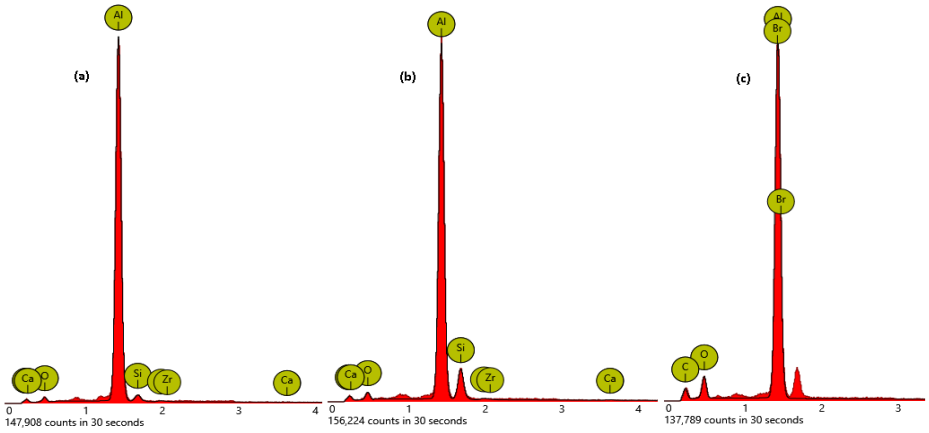

Figure 2: Energy dispersive x-ray spectroscopy for sample (a) 5 (b) 8 (c) Control

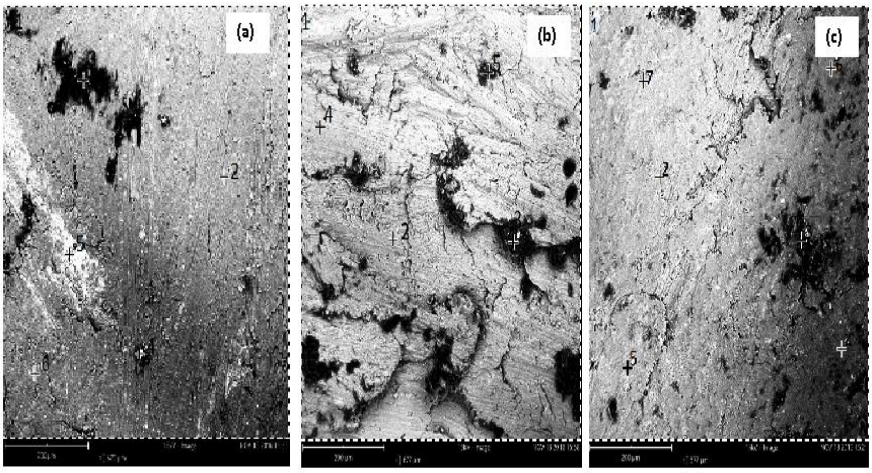

Figure 3: SEM Micrographs of (a) Aluminum alloy + 15% ZrB_2 + 10% Snail shell (Sample 5), (b) Aluminum alloy + 30% ZrB_2 + 0% Snail shell (Sample 8), and (c) 100% New Aluminum alloy (control 1).

Table 5: EDX Legends, Element Symbol and their Confidence Concentration on SEM Micrographs

ALZrBSS5	
Legend	**Element symbol/confidence concentration on EDX**
+1	Al (86.6), Si (3.6), O (7.3) and C (26)
+2	Al (95.5) and Si (4.1)
+3	Al (68.2), C (28.1) and Si (3.8)
+4, +5	Al (100)
+6	Al (95.l (100) 6) and Si (4.5)
ALZrBSS8	
+1	Al (76.7), Si (11.4), O (9.3) and C (2.6)
+2	Al (94.3) and Si (5.7)
+3	Br (100)
+4	Al (85.1) and Si (14.9)
+5	Br (89.9) and O (10.0)
CONTROL 1	
+1	Al (73.0), Si (11.0), C (2.0) and O (13.2)
+2	Al (91.7) and Si (8.3)
+3	Br (45.6), O (35.4), C (6.9), Fe (9.5) and Ca (2.7)
+4	Al (88.2), Si (3.6) and O (8.2)
+5	Al (79.1), Si (6.4) and O (14.5)
+6	Al (96.1) and Si (3.9)
+7	Al (86.4) and Si (13.6)

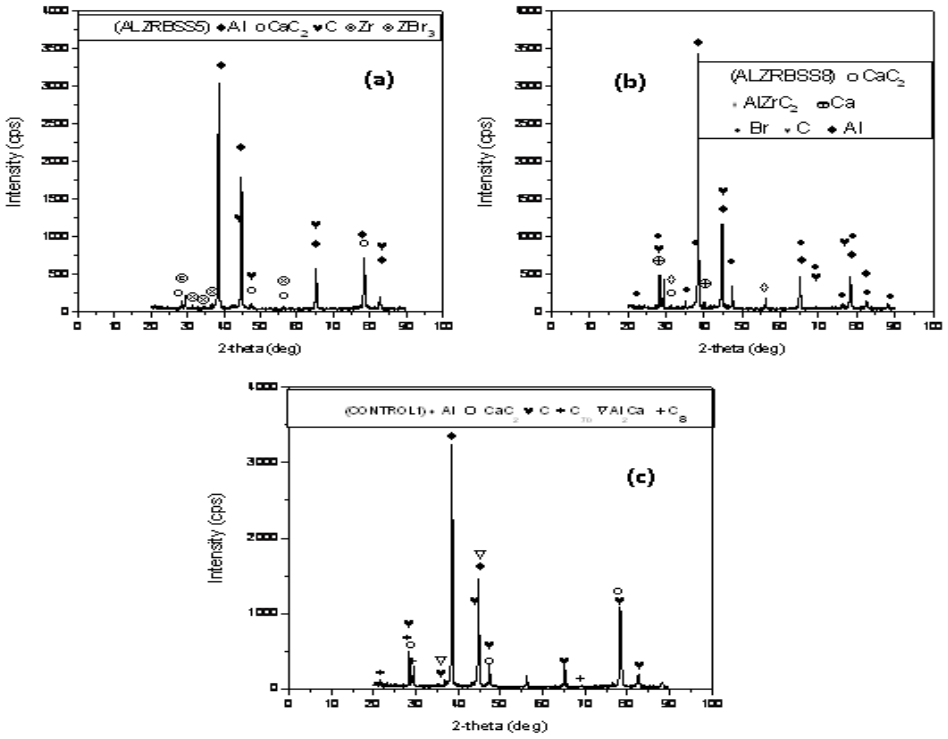

Figure 4: XRD pattern of Aluminum Piston reinforced with Zirconium diboride and Snailshells (a) ALZrB$_2$SS5 (b) ALZrB$_2$SS8 and (c) Control 1

3.5 Microstructure

The SEM images and EDX profiles are shown in Figure 3a, b and c respectively for samples 5, 8and control 1, It shows sample 5 and 8 with their positions indicating the elements contained and their confidence concentration on the SEM micrograph. In sample 5, 8 and control 1, the EDX quantitative analysis of positions 2 reveals a composition rich in Al (95.5, 94.3 and 91.7 wt. %.) and Si (4,1, 5.7 and 8.3 wt. %.) respectively. While, position 3 (black colour) in sample 5 contains 0 wt. %. Br., whereas, position 3 in sample 8 and control 2 reveal a composition rich in Br, 100 wt. %., and 45.6 wt. %. Table 5 shows the element and their confidence concentration as indicated by the legend. The presence of Mg in chemical composition of Al-alloy improves the wettability of ceramics particles with matrix alloy and also increases the retention percentage. As reported by Rana [19] in 2012 and Stadler [20] in 2011 piston alloy primarily contain two types of Al_3Ni phase which are plate-like and needle like morphologies. It was observed that Ni particles are distributed homogeneously in acicular form inside Al-Si matrix without any cracks or voids between them. The reaction of Ni particles with Al matrix forms Al_3Ni intermetalics.

3.6 XRD Results

The XRD of Sample 5 with composition of (Aluminum alloy + 15% ZrB_2 + 10% Snail shells), 8 (Aluminum alloy + 30% ZrB_2 + 0% Snailshells) and the control (100% new piston) are presented in Figure 4. Calcium carbide (CaC_2), zirconium, calcium, carbon and bromine are the major interest and they are found in the peak as revealed by XRD. The entire samples under study have calcium carbide and Aluminum as revealed by XRD. The samples 5 contain zirconium bromide and zirconium (Zr, ZBr_3) while, sample 8 contains aluminum zirconium and bromine ($AlZrC_2$, Br) which are absent in control sample. Moreso, control 1 possesses aluminum calcium, carbon and fellurite (Al_2Ca, C, C_{70}). It can be observed that carbon is present in the entire sample under study. Zirconium diboride has excellent mechanical properties with higher strength and fracture toughness while carbon has high hardness and good shield properties against neutron.

3.7 Fatigue Test Results

The experimental set up used in test bear a close resemblance to the work of Maleque [21]. We clearly observed in this study that with the maximum stress of 1422.6 MPa which was applied to all the composites samples being understudied in this study and from the S-N curve, the results shows that the fatigue life of aluminum alloy reinforced with the composite material increases/decreases as the reinforcement weight fraction of snail shell increases in sample 8, 5 and control 1 accordingly. The increase may be attributed to higher load bearing capacity of the composite material which gives higher yield strength and ultimate tensile strength with lower ductility. Moreover, other samples show a low cycle fatigue life than the unreinforced control sample. This can be as a result of decrease in cyclic ductility which induces brittleness in the fatigue properties [22].

It was observed that the S-N curve (Figure 5) shows that $ALZrB_2SS5$, $ALZrB_2SS8$ and control 1 increase as arranged. We observed that control 1 (new piston) shows highest value, good and high fatigue live properties than the reinforced samples 5 and 8. Considering what played out between sample AlZrBSS 5 and 8, it can be concluded that the presence of reinforcement particles increases on toughness and the fatigue life cycle as reinforcement is increased. However, Prakash and Arun [23] concluded that fatigue behaviour of composite increases with increase in reinforcement but at higher reinforcement there will be much difference in fatigue behaviour. This may be as a result of behavioural change as concluded by Prakash and Arun [23] in which fatigue was also conducted on piston and their result falls into low cycle fatigue live as seen in this research.

Uygur [22] claimed that the presence of reinforcement particle influences the toughness and fatigue life cycle of the composite material. He concluded that low fatigue behaviour under strain controlled cyclic loading condition as compared to unreinforced aluminum alloy is reduced by the addition of hard ceramic particle in aluminum composite material. This reduction is as a result of the brittle nature of ceramic particles phase, high dislocation density at the interfaces, hydrostatic stress development and plastic flow constant within the aluminum alloy.

It is important to note that the fatigue live cycle increases and decreases with increase in reinforcement. It is noted that many non ferrous metal and alloy such as aluminum, magnesium and copper do not exhibit well defined endurance limit, but from power relationship of S - N curve, it is only valid for fatigue live that are on design line. The ranges for ferrous metal are from 1×10^3 to 5×10^8. In a nutshell the fatigue live of the samples analyzed in this study is limited to 1×10^3 cycle which indicates that they have low cycle fatigue live because the type of machine used for this test is low cycle fatigue machine (Avery Denison fatigue, model 7305).

3.8 Impact Energy

The average impact energies of the samples are shown in Figure 6. Sample ALZrBSS5 and ALZrBSS8, with the average strain rate of 0.0049 and 0.0068 %, absorbed an average impact energy of 48 and 66.5 J, respectively while the control sample 1 with an average strain rate of 0.0056, absorbed an average impact energy of 55 J. The average impact energy for samples 5 (48 J) is lower than that of the control 1 (55 J) while that of the sample 8 (66.5 J) is higher than the control 1 (55 J). Meanwhile, the standard deviation for impact energy absorbed was 2.5. The ductility nature of aluminum alloy makes it undergo plastic deformation which is responsible for the high impact energy especially at room temperature in which is experiment was carried. It was observed in modified samples, that ALZrBSS5 (139 MPa, 48 J) has higher yield and lower impact strength than ALZrBSS8 (87 MPa, 66.5 J). It is generally observed from tensile properties that high modulus of resilience depends on the relationship between stress and strain property of a material, a higher ductility is dependent on high stress and strain properties.

The impact energy of a composite is influenced by many factors: including the toughness properties of the reinforcement, the nature of interfacial region and frictional work involved in pulling out the particle from the matrix [24]. The result obtained in this study support the work of Hassan et al [25]; Imosili et al [26] as reported that the impact energy decreases with increment in wt. % of snailshell particles. It reveals that decrease in wt. % of snail shell increases impact energy which is not in support of the work of Genevive et al [27] that the increase in impact of a polymer composite with increase in filler content.

The result of impact energy obtained in this study falls within the range of charpy impact test and fracture toughness of aluminum alloy at room temperature [28]. High impact energy is expected in engineering applications of composites materials. In selecting a suitable material in engineering design, energy to be absorbed by a material should be paramount and not only by usual design parameters [29]. However, it was reported that the only drawback is that as the wt. % of reinforcement increases the impact energy of composite decreases due to the presence of ceramic particles [23]. This drawback is observed here.

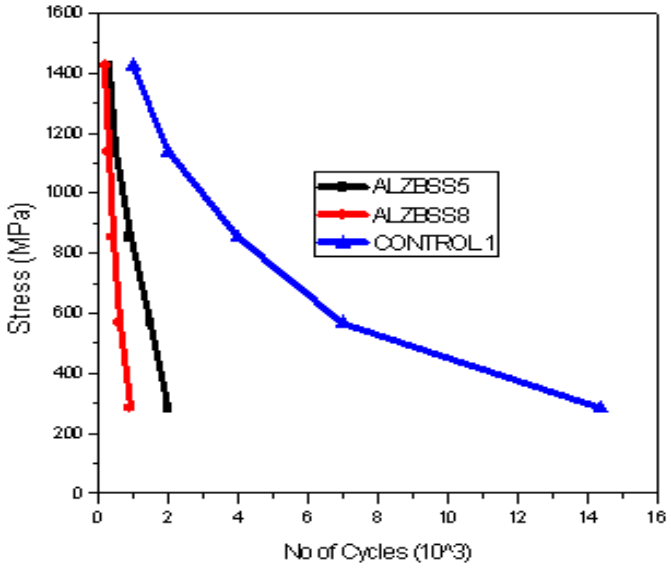

Figure 5: S-N curves for aluminum alloy reinforced with zirconium diboride and snail shells and control sample

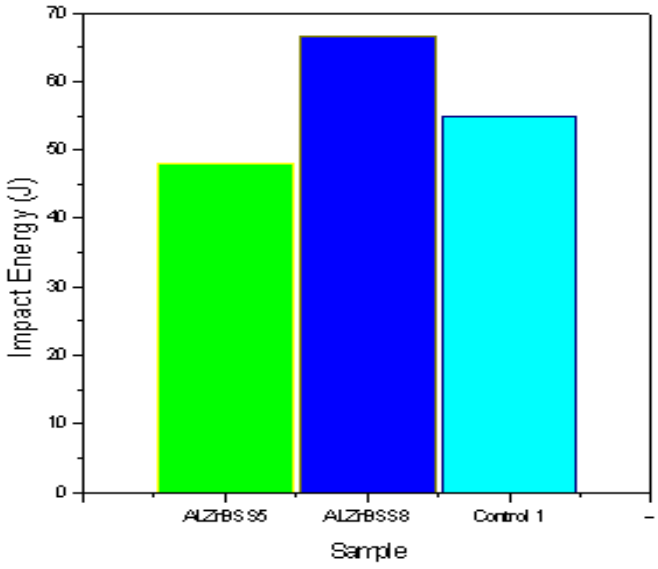

Figure 6: A Chart showing an average Impact Energy for the three samples

3.9 Corrosion Resistance

Figure 7 shows the potentiodynamic curve recorded for three selected samples. The electrochemical parameters such as corrosion potential (E_{corr}), corrosion current density (I_{corr}), anodic Tafel slope, the cathodic Tafel slope and corrosion rate (V_{corr}) are all evaluated in Table 6 with each of their results. Samples ALZrBSS5 and ALZrBSS8 have increase corrosion rate with increase in reinforcement of the aluminum alloy, this corroborated the work of Ferris [30] which concluded that corrosion rate increases with increase in percentage of alumina particles for the given atomized sample in 3.5 % NaCl solution at a temperature of 30 ^{0}C. He attributed it to galvanic corrosion between the matrix and reinforcement and the presence of second phases around Al_2O_3 particle in microstructure of AMCs.

The order of corrosion rate is: Control 1, ALZrBSS8, and ALZrBSS5. From the results of all the samples highlighted above, they have low corrosion rate with slight difference in their value. It is believed that their reaction to corrosion is low which indicated that they have good resistance against corrosion rate. Furthermore, the potential corrosion of the samples increases in the following order; Control 1, ALZrBSS8, and ALZrBSS5. Decrease in corrosion potential (E_{corr}) value indicates the loss of passivity of the sample due to thinning of primary oxide layers by chemical dissolution action. Samples with lower reinforcement content, lower I_{corr} and less negative potential, is attributed to lower reinforcement content in the same alloy matrix which reduces the cathodic area to localized regions such as impurities, porosities and reinforcements in the alloy matrix.

Similar results were obtained for all samples showing increase in corrosion current values which indicate that the composite in them undergo more. Control 1 (new piston) tend to have low (decrease) corrosion potential, this indicated that corrosion rate of base alloy is lower than the composite, which means the clean surface of the base alloy reaches to the passivity rapidly when exposed to oxygen containing the environment forming particle oxide film Al_2O_3 which is good adherence to metal surface and poor conductivity for change transfer. Base alloy exhibit less susceptivity to pitting corrosion, this indicated that new piston (control 1) with no reinforcement has the lowest corrosion rate.

Table 6. Result of Tafel Polarization and the electrochemical studies on corrosion of Aluminum alloy

S/N	Sample	Corrosion Rate (mmpy)	Corrosion Potential (E_{cor})	Corrosion Current (Icor) µA	Cathodic Tafel Slope mV	Anodic Tafel Slope mV
1	ALZRBSS5	0.19486	-584.300	-17.902	2.34E+3	60.608
2	ALZRBSS8	0.12416	-586.271	-11.407	496.622	42.303
3	Control 1	0.11808	-660.509	-11.652	591.732	120.876

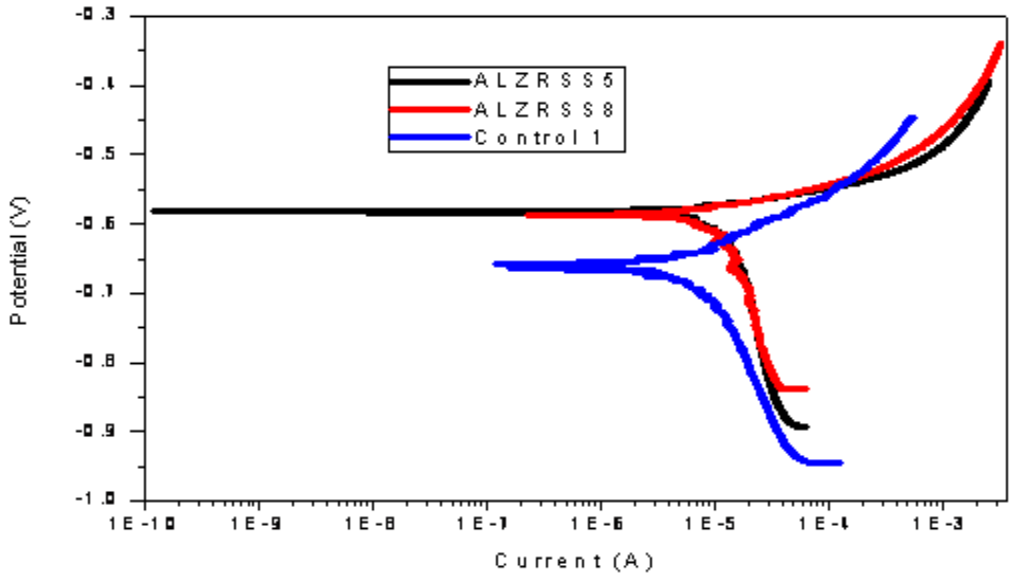

Figure 7: The Tafel plots of Potential difference against Current

Olawuni et al.,

It is reported that one of the major disadvantages of particulate reinforced with MMCs is the influence of reinforcement on the corrosion resistance as large content of reinforcement at the surface of composite accelerate the pit growing into metal [31]. According to Emergul and Aksut [32] aluminum and its alloy exhibits high corrosion rate in solution containing aggressive anions or highly alkaline solution and chlorides. He concluded that when aluminum metal is immersed in alkaline solution the alumina layer rapidly dissolves due to chemical dissolution. An increase in iron content will lead to the promotion of pitting corrosion. However, the presence of appreciable amount of soluble alloying elements such as copper, magnesium, silicon and zinc will make these alloys susceptible to stress-corrosion cracking.

According to Lee and Kim [33] the corrosion of aluminum and aluminum alloy in the alkaline medium can be explained on the basis that the surface of the material are covered by passive film of alumina formed by the reaction of aluminum with air. Uhlig and Revie [34] concluded that the corrosion behaviour of aluminum is sensitive to small amount of impurities (or alloying elements) in the metal, all these impurities, with the exception of magnesium; tend to be cathodic aluminum. The content of silicon, iron and nickel play a major role in corrosion properties. It was reported earlier that silicon is an important parameter affecting mechanical properties and corrosion resistance while high content of iron increases pitting corrosion.

4. CONCLUSION

It has been demonstrated in this study that zirconium diboride and snail shells has a great effect in development of piston material. The parameter obtained through D-Optimality technique which was used for optimization for further characterization has proven that the mechanical properties of the result obtained with the composite materials are better than the work that has been carried out in this area with better mechanical properties. Moreover, dry sliding wear behaviour of Aluminum alloy of As-cast and reinforced using pin-on-disc under a static load and varying sliding distance have been successfully analyzed by using the Taguchi design of experiment to calculate minimum specific wear rate and it shows that wear loss is greatly reduced or minimized and mechanical properties is improved.

It is paramount to note that there was no trend in the parameters obtained in this study because design of experiment (D-optimality technique was used to determine the mixing composition unlike others which varying parameters were used for their mixture ratio. Meanwhile, the result shows that hardness, yield point and tensile strength increases with increase in snail shells particles to aluminum alloy. Moreso, the use of zirconium diboride which is a ceramic material with high melting temperature also play a great role in reinforcement. It is clearly observed that composite material has a greater influence on waste piston material and it has been displayed in this study how it can be used to improve mechanical properties of a material.

Based on the findings in this study, it is concluded that the potentiodynamic polarization and electrochemical studies showed that corrosion rate of the composite is higher than that of base alloy (new piston). It is still important to know that discarded piston contained different alloy because it was collected at random and is made by different manufacturer.

REFERENCES

[1]. Smith, F.W., Hashemi, J., 2006. Foundation of Material Science and Engineering, Mcgraws-Hill Book, 4th Edition.

[2]. Lide, R., 2004. Handbook of Chemistry and Physics, Properties of Aluminium and its Alloy. 85th Edition, CRC Press, P. 2712.

[3]. Piston Ring Handbook Federal-Mogul Burscheid GmbH., 2008. Federal Mogul Corporation.

[4]. Khruschor, M.M., 1974. Principle of abrasive wear. Wear, 28: 69-88.

[5]. Garrison Jr, W.M., 1987. Abrasive Wear Resistance. The Effect of Ploughing and the Removal of Ploughed Material. Wear, 114: 239-247.

[6]. Silva, F.S., 2006. Fatigue on engine piston-A Compedium of case studies. Engineering Failure Analysis, 13: 480-492

[7]. Joyce, M.R., Style, C.M., 2003. Reed PA. Elevated temperature-short crack fatigue behaviour in near eutectic Al-Si alloys. Int. J. Fatigue, 25: 863-9.

[8]. Priest, M., Taylor, C.M., 2000. Automobile engine tribology-approaching the surface wear, 241 (2): 193-203.

[9]. Mahesha, N.S., Hanumantharaya, R., Mahesh, B.D., 2006. Ramakrishna, D.P. Shivakumar, K.M. Tribological wear behaviour of AlSl 60 (17-4PH) stainless steel hardened by precipitation hardening. American Journal of Material Science, 6 (4A): 6-14.

[10]. Hemanth, T.R., Swampy, R.P., Khardrashekar, T.K., 2013. An experimental investigation on wear parameters of metal matrix composite using taguchi technique. India Journal of Engineering and Material Science, 20: 329-333.

[11]. Jato, E.O., Asia, I.O., Egbon, E.E., Otutu, J.O., Chukwuedo, M.O., Ewansiha, C.J. 2010. Treatment of Waste Water from Food Industry using Snail Shell.

[12]. Asafa, T.B., Durowoju, M.O., Oyewole, A.A., Solomon, S.O., Adegoke, R.M., Aremu, O.J., 2015. Potentials of snail shells as reinforcement for discarded aluminum based materials. International Journal of Advanced Science and Technology, 84: 1-8.

[13]. Toptan, F., Kerti, I., Rocha, L.A., 2013. Reciprocal dry sliding wear behaviour of B_4Cp Reinforced Aluminum Alloy Matrix Composites, 290-291; 74-85

[14]. Durowoju, M.O., Babatunde, I.A., 2014. Effect of Antimony on the Tensile strength and the Morphology of Si Platelets in Recycled Aluminium Piston Alloys. Journal Material Science Engineering, 3:137.

[15]. Durowoju, M.O., Babatunde, I.A., 2012. Modification of recycled Al-332 alloy using manganese dioxide. International Journal of Engineering Research and Applications, 4:153-162.
[16]. Saka, N., Pamies-Teixeeira, J.J., Suh, N.P., 1977. Wear of two-phase metals. Wear, 44: 77-86.
[17]. Suresha, B., Siddaramaiah, S., Kishorec, S., Sampath, K.P., 2011. Wear behaviour of graphite illed glass epoxy composites. Wear, 267: 1405.
[18]. Agunsoye, J.O., Talabi, S.I., Aigbodion, V.S., Olumuyiwa, A., 2013. Effects of silica ceramics particle sizes on the properties of recycled polyethylene composites. Advances in Natural Science, 6: 1-8.
[19]. Rana, R.S., Purohit, R., Das, S., 2012. Reviews on the influences of alloying elements on the microstructure and mechanical properties of aluminum alloys and composites. International Journal of Scientific & Research Publication, 2: 1-7
[20]. Stadler, F., Antrekowitsch, H., Fragner, W., Kaufmann, H., Uggowitzer, P.J., 2011. The effect of Ni on the High Temperature Strength of Al-Si Cast Alloys. Material Science Forum, 690: 274-277
[21]. Maleque, M.A., Adebisi, A.A., Izzati., 2016. Analysis of Fracture Mechanisim for Al-Mg/SiCp Composite Materials. International Conference on Mechanical, Automotive and Aerospace Engineering. Material Science and Engineering, 184: 012031.
[22]. Uygur, I., 2002. Low Cyclic Fatigue Properties of 2124/SiC_2 Al-Alloy Composites. Turkish Journal of Engineering, Environmental Science, 26: 265-274.
[23]. Prakash G, Arun LR. Characterisation of Aluminum Flyash-Alumina Composite for Piston Analysis by CAE TOOLS. International Journal of Innovative Research in science Engineering and Technology; 2013.
[24]. Atuanya, C.U., Edokpia, R.O., Aigbodion, V.S., 2014. The Physio-Mechanical Properties of Low Density Polyethylene (RLDPE) / Bean Pod Ash Particulate Composites. Results Phys, 4: 88-95.
[25]. Hassan, S.B., Ogbenevweta, J.E., Aigbodion, V.S., 2012. Morphological and Mechanical properties of Carbonized Waste Maize Stalk as Reinforcement for Eco-Composites Part B. 43: 2230-2236.
[26]. Imoisili, P.E., Ezenwafor, T.C., Attah-Daniel, B.E., Olusunle, S.O., 2013. Mechanical properties of cocoa-pod/epoxy composite; effect of filler fraction. Am Chem Sci. 4: 526-531.
[27]. Genevive, C., Onuegbu, I., Ogbennaya, I., 2011. The effects of filler contents and particle sizes on the mechanical and end-use properties of snail shell powder filled polypropylene. Material Science and Application, 2: 811-817.
[28]. Marrow, J., 2014. The Charpy Impact Test and Fracture Toughness. Fracture Energy versus Temperature for various Metals. Metal source Journal, University of Manchester, U.K.
[30]. Farris, A.S., 2009. Development of 7020 Al-Al2O3 Composite by Atomization and Stir Casting Processes" PhD Thesis, School of Applied Sciences, University of Technology, Baghdad.
[31]. Dahrzanski, I.A., Wladarczk, A., Adamiak, M., 2005. Structure Properties and Corrosion Resistance of PM Composite Matrix Based on ENAW-212 Aluminum Alloys Reinforced with Al_2O_3 Ceramic Particle. Journal of Material Processing Technology, 162-163: 27-31.
[32]. Emergul, K.L., Aksut, A., 2000. The behaviour of aluminum in alkaline media. Corrosion Science, 2051-2067.
[33]. Lee, K.K., Kim, K.B., 2001. Electrochemical impedance characteristics of pure Al and Al-Si Alloy in NaoH solution. Corr. Sci. 43: 561-575.
[34]. Uhlig, H.H., Revie, R.W., 2008. Corrosion and Corrosion Control; An Introduction to Corrosion Science and Engineering, 4th Edition.